Annals of Applied Microbiology & Biotechnology Journal ISSN: 2576-5426

Research Article

Protection by Resveratrol against DEHP-Induced Testicular Cellular Senescence is Mediated by Inhibiting PTEN Loss

Xinyu Yan[1], Qing Tian[1], Jiawei Xu[1], Jiaxuan Ma[1], Xiance Sun[2], Jing Li[3], Ningning Wang[1], Xiaofeng Yao[2], Tianming Qiu[2], Cong Zhang[1], Haoyuan Deng[1], and Guang Yang[1*]

[1]Department of Food Nutrition and Safety, Dalian Medical University, China

[2]Department of Occupational & Environmental Health, Dalian Medical University, China

[3]Department of Pathology, Dalian Medical University, China

Abstract

Di(2-ethylhexyl) phthalate (DEHP) is recognized as an endocrine-disrupting compound and is widely adopted as a plasticizer. Evidence links its reproductive toxicity to the tumor suppressor PTEN, genomic stability is crucially maintained by DNA damage repair (DDR). PTEN loss promotes DNA damage accumulation and cellular senescence. Resveratrol (RES), a natural polyphenol, exhibits antioxidant and anti-inflammatory activities and shows protective potential for the male urogenital system. Nevertheless, the mechanisms associated with testicular senescence due to DEHP exposure and RES protection remain incompletely understood. This study employed in vivo and in vitro models, including cell viability assays, testosterone ELISA, cell cycle distribution analysis, senescence marker staining, Western blotting, and PTEN modulation. DEHP exposure significantly reduced testosterone levels in rat testis and TM3 cells, which was ameliorated by RES. DEHP/MEHP treatment upregulated senescence markers (β-Gal, p21, p16, γH2AX), downregulated PTEN and CDK2, and increased p-CHK2. These changes were reversed by RES. PTEN overexpression attenuated MEHP-induced senescence, G1 arrest, and testosterone reduction, while PTEN inhibition abolished RES protection. These findings elucidate the mechanism by which RES protects against DEHP-induced senescence via inhibiting PTEN loss.

Keywords: Resveratrol; Di(2-ethylhexyl) phthalate; Cellular Senescence; PTEN Loss; Testicular Toxicity.

INTRODUCTION

As a class of synthetic chemicals, phthalates (PAEs) are extensively employed as plasticizers, particularly in polyvinyl chloride (PVC) products. Due to their non-covalent binding to plastic polymers, the migration of these compounds into the environment underlies pervasive human contact and classification as typical endocrine disruptors [1,2]. Among PAEs, DEHP is one of the most representative and is commonly detected in medical devices, food packaging, and construction materials [3,4]. The primary routes of human exposure to DEHP include ingestion, inhalation, and dermal absorption, posing potential health risks that include reproductive and developmental toxicity, hepatotoxicity, and carcinogenicity [5,6]. In males, DEHP exposure impairs Sertoli and Leydig cell function, causes functional impairment of the blood-testis barrier, causes spermatogenic failure, and contributes to testosterone deficiency [7,8]. In females, it interferes with follicular development, steroid hormone synthesis, ovarian reserve, and the estrous cycle [9].

Submitted: 23 January, 2026 | **Accepted:** 03 March, 2026 | **Published:** 07 March, 2026

***Corresponding author:** Guang Yang, Department of Food Nutrition and Safety, Dalian Medical University, China

Citation: Yan X, Tian Q, Xu J, Ma J, Yang G (2026) Protection by Resveratrol against DEHP-Induced Testicular Cellular Senescence is Mediated by Inhibiting PTEN Loss. Ann Appl Microbiol Biotechnol J 8: 10.

In vivo, Mono(2-ethylhexyl) phthalate (MEHP) generated upon DEHP exposure, which is the principal metabolite via hydrolysis catalyzed by esterases [10]. MEHP surpasses DEHP in both polarity and biological activity, establishing it as the key effector in mediating DEHP-induced reproductive toxicity [11,12]. Therefore, investigating the toxicological mechanisms of MEHP is essential for understanding the health risks of phthalate exposure.

Cellular senescence entails an irreversible cessation of cell proliferation, representing a fundamental physiological response to various stressors [13,14]. The injuries accrual of senescent cells is mechanistically correlated with organismal aging and the pathogenesis mechanism of representative age-related diseases, notably atherosclerosis and neurodegenerative disorders [15,16]. The senescence-associated secretory phenotype (SASP) of accumulated Sertoli and Leydig cells impairs testicular function by disrupting the blood-testis barrier and fostering inflammation, thereby contributing to reproductive decline [17,18]. Consequently, the emergence of senolytic therapies, which target senescent cells for removal, represents a promising strategic development in the mitigation of aging and linked pathological conditions [19,20].

Studies indicate that DEHP promotes cellular senescence through multiple mechanisms. It induces oxidative stress, leading to triggering of the p53-p21 and p16-pRb signaling pathways and subsequent proliferative arrest [21,22]. DEHP also causes DNA double-strand breaks (DSBs), initiating DDR marked by γH2AX formation and triggering senescence [23,24]. Furthermore, DEHP downregulates PTEN expression, resulting in hyperactivation of the PI3K/AKT pathway and potentially accelerating telomere dysfunction [25,26].

Within the testis, DEHP preferentially triggers senescence in somatic cells, namely Sertoli and Leydig cells. This action disrupts the spermatogenic niche and impairs testosterone production, forming a central mechanism of its reproductive toxicity [27].

PTEN loss is characterized by the impairment or absence of PTEN tumor suppressor function due to genetic mutations, deletions, epigenetic silencing, or post-translational degradation [28]. Serving as a pivotal repressor within the PI3K/AKT/mTOR network, PTEN loss leads to aberrant PIP3 accumulation, persistent AKT activation, and promotion of tumorigenesis through enhanced proliferation, suppressed apoptosis, angiogenesis, and invasion [29,30]. Nuclear PTEN also contributes to maintaining genomic stability through involvement in DNA repair mechanisms, deficiency in this factor is associated with compromised genomic integrity and increased mutagenesis [31,32].

RES, a natural polyphenolic stilbene found in grape skins, red wine, peanuts, and Polygonum cuspidatum, is widely used in dietary supplements [33]. The compound's diverse pharmacological actions include antioxidant and anti-inflammatory effects, protection against cardiovascular and neurological damage, and potential inhibition of cancer development [34]. Under the framework of cellular senescence, RES has been demonstrated to counteract aging by reducing oxidative stress and suppressing inflammation [35]. Notably, RES can upregulate or stabilize PTEN expression and activity, thereby preserving PTEN-mediated tumor suppressor signaling and offering protection against senescence [36,37].

This research integrates evidence from both animal studies and cellular experiments, which were employed to examine whether RES protects against DEHP-induced testicular cellular senescence by counteracting PTEN loss. The involvement of the PTEN/p-CHK2/CDK2 pathway in DEHP-mediated senescence was investigated, and the protective role of RES in this context was elucidated.

MATERIALS AND METHODS

Animals Model

SPF male Sprague-Dawley rats at 3 weeks of age (postnatal day 21) were procured from the Institute of Genome Engineered Animal Models for Human Disease at Dalian Medical University. A standardized one-week acclimatization protocol was implemented under controlled laboratory conditions preceding experimental interventions. All rats were housed in a SPF environment with controlled conditions: a 12-h light/dark photoperiod, temperature maintained at 25 ± 2 °C, and humidity at 50 ± 5%. Animals had ad libitum access to standard rodent diet and water. DEHP (≥98% purity, Alfa Aesar, USA) was prepared as a suspension in corn oil at a concentration of 500 mg/kg body weight and administered via oral gavage at a volume of 4 mL/kg. RES (Solarbio, China) was initially dissolved in DMSO to generate a 100 mM stock solution, subsequently diluted with sterile physiological saline to the desired working concentration for *in vivo* administration.

A randomized grouping design was employed, resulting in four experimental cohorts of equal size (n = 8 per group): (I) Control group: gavaged with corn oil and intraperitoneally injected with saline for 3 months. (II) DEHP group: gavaged with DEHP (500 mg/kg/day) and intraperitoneally injected with physiological saline for 3 months. (III) DEHP+RES group: gavaged with DEHP (500 mg/kg/day) and intraperitoneally injected with RES (60 mg/kg/day) for 3 months. (IV) RES group: gavaged with corn oil and administered via intraperitoneal injection with RES (60 mg/kg/day) for 3 months. Following a 24-hour interval after the final administration, rats were euthanized under deep anesthesia induced by pentobarbital humanely. Testicular tissues were promptly excised and preserved for subsequent analytical procedures.

Cell Culture and Treatment

The TM3 mouse Leydig cell line was obtained from the National Collection of Authenticated Cell Cultures, was cultured in DMEM/F12 medium containing 2.5% fetal bovine serum, 5% horse serum, and 1% penicillin/streptomycin, and maintained at 37 °C in a humidified incubator with 5% CO_2.

Stock solutions were prepared by dissolving MEHP (MCE, USA; 55.67 mg) and RES (2.2824 mg) in 1 mL of DMSO to achieve final concentrations of 200 mM and 10 mM, respectively. Cells in the MEHP group were exposed to 0 or 200 μM MEHP for 24 h. Cells were simultaneously treated with 200 μM MEHP and 2.5 μM RES for an equivalent period in protection experiments.

Cell Viability Assay

TM3 cells were seeded in 96-well plates at a density of 5,000 cells per well and exposed to MEHP (0 or 200 μM) along with a gradient of RES concentrations (0–40 μM) for 24 hours to assess viability. Following the manufacturer's protocol, 10 μL of CCK-8 reagent was added to each well, and then the absorbance at 450 nm was measured with a microplate reader. The relative cell survival rate was then determined based on the obtained readings.

Testosterone Content Assay

Testosterone concentrations in testicular tissue homogenates and TM3 cell culture supernatants were quantified using a commercially available Rat Testosterone ELISA Kit (BPE30610, Lengton, China). For tissue specimens, 40 μL of each standard or sample was loaded into the wells, after which horseradish peroxidase (HRP) and biotin-conjugated detection antibodies were added sequentially, followed by incubation at 37°C for 1 hour. After thorough washing, the chromogenic substrate was added and cultured at 37°C for 10 minutes, and the absorbance was subsequently measured at 450 nm. Based on the OD values of the known standards, a standard curve was generated. For cell culture supernatants, the medium was clarified by centrifugation at 4°C and 3600 rpm for 5 minutes, and the resultant supernatant was subjected to the same assay procedure.

Flow Cytometry for Cell Cycle

Flow cytometry was used to assess the cell cycle distribution by using a commercially available Cell Cycle and Apoptosis Analysis Kit (PI staining) (HY-K1071, MCE, USA). Briefly, TM3 cells treated with MEHP (0 or 200 μM) and RES (0 or 2.5 μM) for 24 hours were detached, fixed with pre-chilled 70% ethanol for 24 hours, and subsequently stained with propidium iodide (PI) working solution. With an excitation wavelength of 488 nm following incubation at 37°C in the dark for 30 minutes cells were subjected to flow cytometric analysis. By using FlowJo software, data were processed and quantified.

SA-β-Gal Stain

Senescence-Associated β-Galactosidase (SA-β-Gal) Staining Kit (G1580, Solarbio, China) was used to evaluate cellular senescence. TM3 cells were seeded into 6-well plates at 2.5×10^4 cells/well and subsequently exposed to MEHP (0 or 200 μM) and RES (0 or 2.5 μM) for a period of 24 hours. Cells were fixed using the supplied β-Gal fixative for 15 min at room temperature after treatment, rinsed three times with PBS, and then incubated with the staining working solution overnight (12–24 h) at 37°C. Cells exhibiting blue cytoplasmic staining, indicative of SA-β-Gal positivity, were observed and manually counted using an inverted light microscope.

Western Blotting

Total protein was extracted from rat testicular tissues and TM3 cells using a commercial extraction kit (Beyotime, China). Protein concentration was quantified using the bicinchoninic acid (BCA) method. Protein samples were resolved by SDS-PAGE and transferred to PVDF membranes (IPVH00010, Merck Millipore, USA). Membranes were blocked with 10% skim milk for 1.5 h, then incubated with primary antibodies overnight at 4°C. Following TBST washes, membranes were incubated with HRP-

conjugated secondary antibodies. Protein bands were detected with an Omni-ECL chemiluminescence kit (SQ201, EpiZyme, China) and captured using a Bio-Rad ChemiDoc MP imaging system.

The antibodies used included: PTEN (AF5447, 1:1000), β-Gal (WL03124, 1:500), p-CHK2 (AF3036, 1:1000), CDK2 (AF6237, 1:1000), p21 (WL0362, 1:500), p16 (WL01418, 1:500), γH2AX (AF3187, 1:1000), and β-actin (TA-09, 1:5000).

Secondary antibodies were HRP-conjugated Goat Anti-Rabbit IgG (SA00001-2, 1:5000) and HRP-conjugated Goat Anti-Mouse IgG (SA00001-1, 1:5000).

Cell Transfection

According to the manufacturer's instructions, stable PTEN overexpression in TM3 cells was established via transfection with either the pcPten3.1(+) plasmid or the corresponding empty vector pcR3.1 (GenePharma, China), using Lipofectamine™ 3000 transfection reagent (L3000008, Invitrogen, USA) . Transfection was performed 24 hours prior to treatment with MEHP (200 μM) and RES (2.5 μM). Successful overexpression was validated by Western blot analysis.

PTEN Inhibition

VO-Ohpic trihydrate, a PTEN inhibitor (IC50 35 nM), was used. TM3 cells were pretreated with VO-Ohpic (1 μM) for 24 hours prior to co-exposure with MEHP (200 μM) and RES (2.5 μM). A 1 mM stock solution of VO-Ohpic (CAS NO: 476310-60-8, TargetMol, USA) was prepared by dissolving 1 mg of the compound in 2.4085 mL of DMSO. Inhibition efficacy was confirmed by Western blotting.

Statistical Analysis

All quantitative results are presented as mean ± SEM. Statistical comparisons were performed using one-way ANOVA, with each experiment replicated at least three times. Differences were considered statistically significant at $P < 0.05$. GraphPad Prism software was used for all statistical analyses and figure generation.

RESULTS

Protective effects of RESagainst DEHP-induced senescence in rat testicles

Based on prior KEGG analysis indicating DEHP might induce testicular senescence (Zhang H et al., 2024), this study evaluated whether DEHP causes senescence and if RES offers protection. Examination of rat testicular cells revealed that RES conferred protection against senescence induced by DEHP (Figure 1).

Specifically, in the DEHP group relative to controls, testosterone levels were significantly decreased, whereas a marked recovery was observed in the DEHP+RES co-treatment group (Figure 1A). Western blotting revealed that DEHP treatment significantly upregulated senescence-related proteins (β-Gal, p21, p16, γH2AX) in testicular tissue, changes that were reversed by RES co-treatment (Figure 1B, C). To investigate PTEN's role, expression levels of PTEN, p-CHK2, and CDK2 were assessed. DEHP treatment reduced PTEN and CDK2 protein expression while increasing p-CHK2 levels, effects that were reversed by RES (Figure 2B, C).

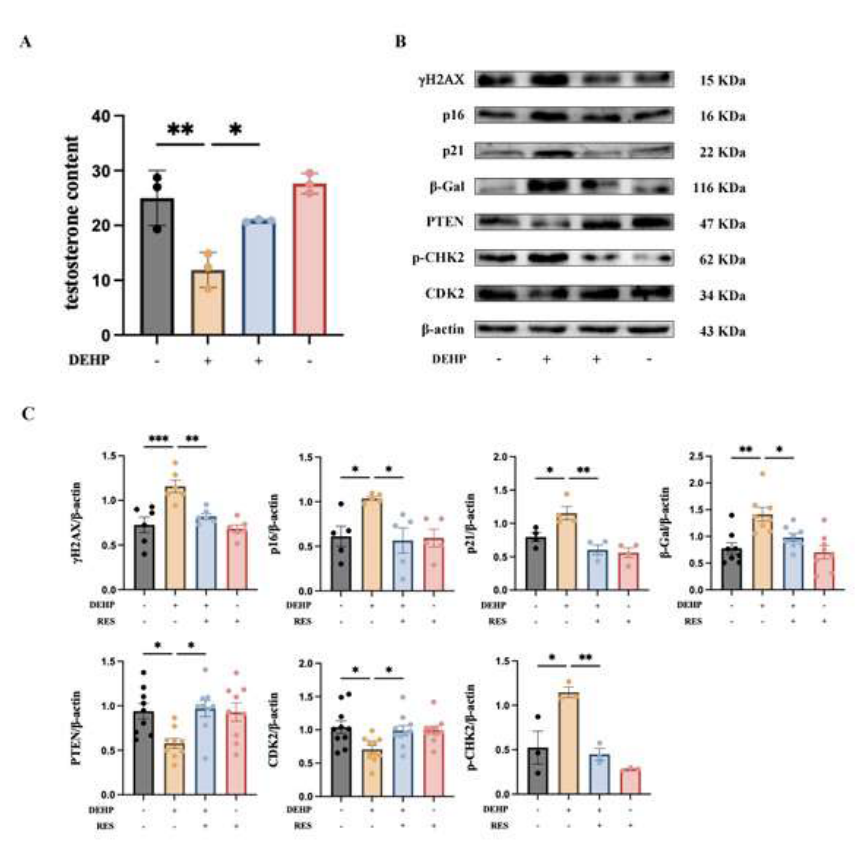

Figure 1: Protective effects of RES against DEHP-triggered senescence in rat testicles. Male Sprague-Dawley rats were received DEHP (0, 500 mg/kg) via gavage and intraperitoneally injected with RES (60 mg/kg/day) for 3 months. **(A)** Evaluation of testosterone levels in testicular tissues. **(B, C)** Analysis of the expressions of relevant effect and signaling pathway proteins subsequent to DEHP and RES treatment in testicular tissues. The results are presented as mean±SEM. *P< 0.05, **P< 0.001, ***P< 0.0001.

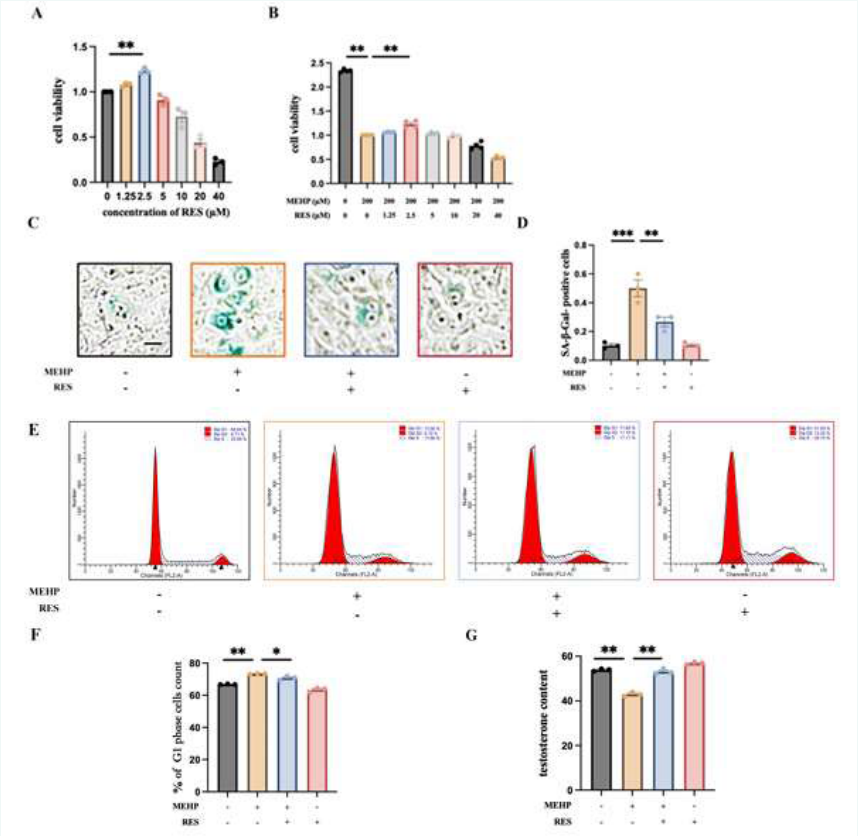

Figure 2: Protective effects of RES against MEHP-triggered senescence in TM3 cells. The cells were processed to 200 μM MEHP and 2.5 μM RES for 24 h. **(A)** Effect of RES on cell viability. **(B)** Effect of MEHP and RES on cell viability. **(C)** Evaluation of testosterone levels in TM3 cells culture supernatant. **(D, E)** The cell cycle distribution of TM3 cells. (F, G) SA-β-Gal stain results of TM3 cells (scale bar: 50 μm). The results are presented as mean±SEM. *P < 0.05, **P < 0.001, ***P < 0.0001. The results in E are presented as **P< 0.001 vs. control group, ##P< 0.001 vs. MEHP group.

Protective effects of RES against MEHP-induced senescence in TM3 cells

TM3 cells were exposed to MEHP in combination with a range of RES concentrations to further investigate the underlying mechanism. CCK-8 assays indicated that 1.25 μM and 2.5 μM RES exhibited no significant cytotoxicity, with 2.5 μM showing maximal protective efficacy (Figure 2A, B). Thus, 2.5 μM RES was used for subsequent experiments.

A gold-standard assay for senescence detection--SA-β-Gal staining, revealed a significant increase in SA-β-Gal-positive TM3 cells following MEHP treatment compared to controls. This increase was substantially attenuated upon co-treatment with RES (Figure 2C, D). Flow cytometric analysis of cell cycle distribution demonstrated that MEHP treatment led to a significant accumulation of G1 phase cells, indicative of cell cycle arrest. This arrest was notably alleviated by concurrent RES administration (Figure 2E, F). Testosterone levels in the supernatant were significantly reduced by MEHP but notably recovered with RES co-treatment (Figure 2G).

MEHP induced senescence in TM3 via PTEN loss

TM3 cells were transfected with a PTEN overexpression plasmid to investigate PTEN's role (Figure 3A, B). Cell viability assessment showed that MEHP significantly reduced viability compared to controls, whereas PTEN overexpression markedly restored viability levels (Figure 3C). An effect that was substantially attenuated by PTEN overexpression, SA-β-Gal staining demonstrated that MEHP treatment significantly elevated the proportion of SA-β-Gal-positive cells (Figure 3D, E). Flow cytometry revealed that MEHP-induced G1 phase arrest was substantially attenuated by PTEN overexpression (Figure 3F, G). Testosterone levels in supernatants, significantly reduced by MEHP, were markedly restored by PTEN overexpression (Figure 3H). Western blotting confirmed that MEHP upregulated β-Gal, p21, p16, and γH2AX, alterations reversed by PTEN overexpression (Figure 3I, J).

MEHP triggered senescence in TM3 cells via PTEN–p-CHK2–CDK2 pathway

To investigate pathway involvement, PTEN-overexpressing TM3 cells were analyzed. Western blotting results aligned with *in vivo* findings: MEHP treatment reduced PTEN and CDK2 protein expression while increasing p-CHK2; these effects were reversed by using PTEN overexpression (Figure 4A-D). In mediating MEHP-induced cellular senescence, these findings underscore the essential role of PTEN. Overexpression of PTEN alleviated senescent effects. In summary, MEHP exposure induces PTEN loss, which downregulates p-CHK2 and subsequently upregulates CDK2 expression, ultimately triggering cellular senescence.

The protective effect of RES against MEHP-induced PTEN loss and senescence in TM3 cells

TM3 cells were pretreated with the specific PTEN inhibitor VO-Ohpic prior to subsequent exposures to ascertain whether the protective effect of RES is dependent on PTEN (Figure 5A, B). Cell viability was significantly impaired in the VO-Ohpic-pretreated group relative to the MEHP+RES co-

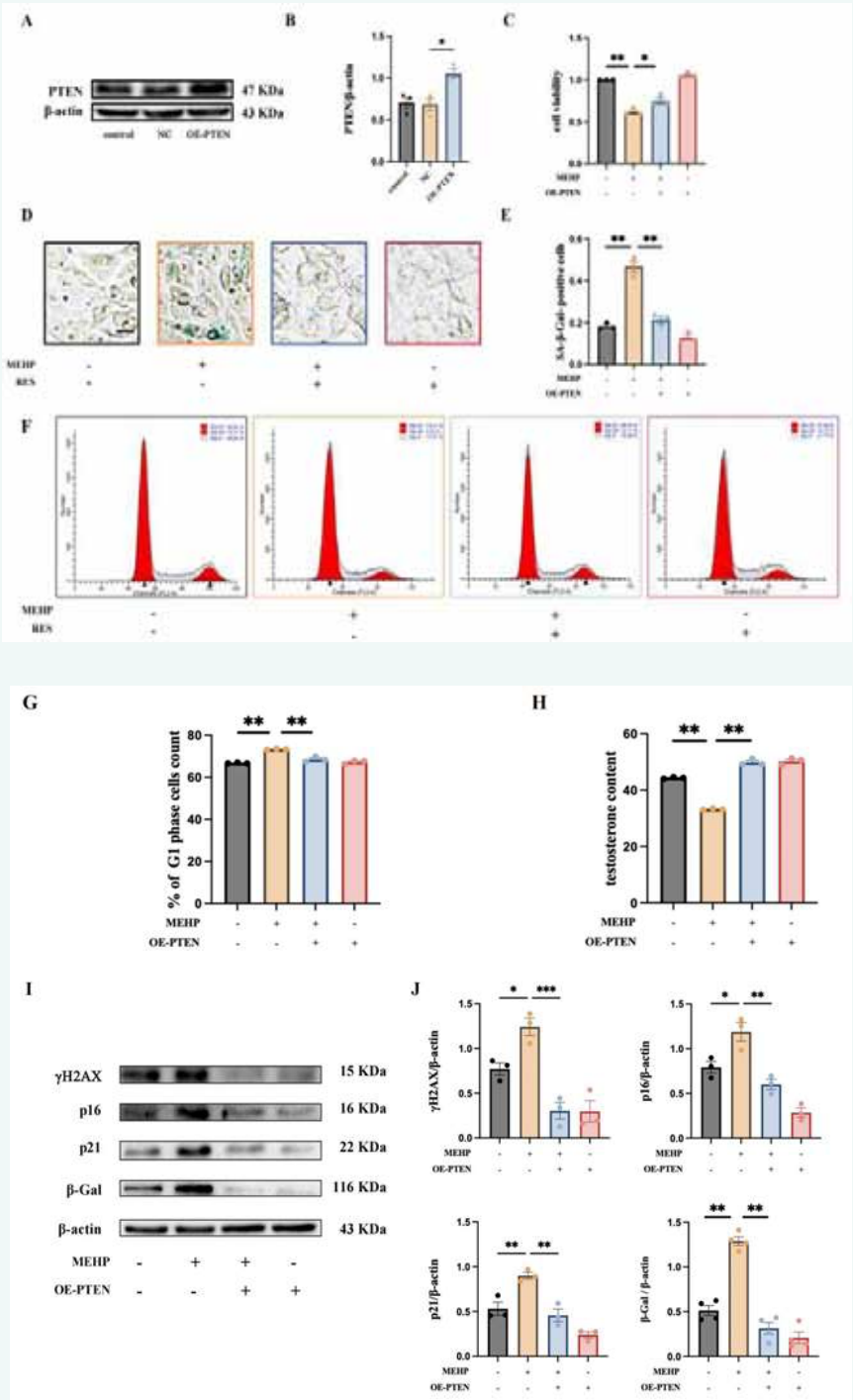

Figure 3: Overexpression of PTEN alleviated MEHP-induced senescence in TM3 cells. The cells were processed to overexpression of PTEN and 200 μM MEHP for 24h. **(A, B)** Analysis of the expressions of PTEN proteins after 24 h overexpression in TM3 cells. **(C)** Effect of overexpression of PTEN and MEHP on cell viability. (**D)** Evaluation of testosterone levels in TM3 cells culture supernatant. **(E, F)** The cell cycle distribution of TM3 cells. **(G, H)** SA-β-Gal stain results of TM3 cells (scale bar: 50 μm). **(I, J)** Analysis of the expressions of relevant senescence proteins in TM3 cells. The results are presented as mean±SEM.*P< 0.05, **P< 0.001, ***P< 0.0001. The results in F are presented as **P < 0.001 vs. control group, ##P < 0.001 vs. MEHP group.

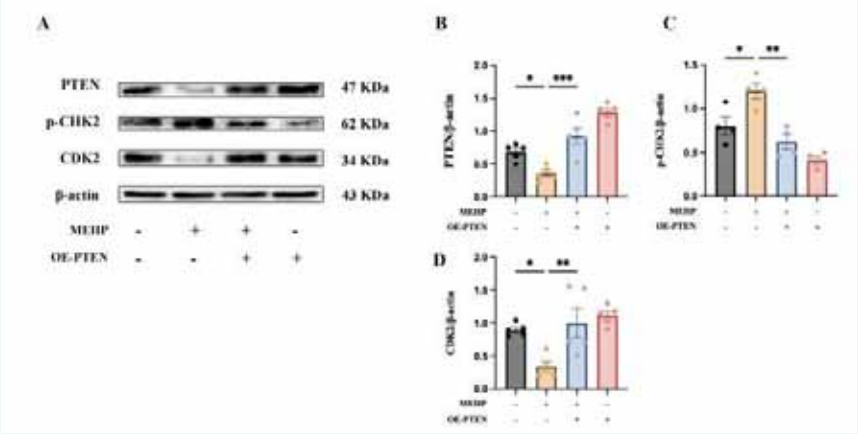

Figure 4: Overexpression of PTEN alleviated MEHP-induced senescence in TM3 cells. The cells were processed to overexpression of PTEN and 200 μM MEHP for 24h. **(A, B)** Analysis of the expressions of relevant signaling pathway proteins in TM3 cells. The results are presented as mean±SEM. *P< 0.05, **P< 0.001, ***P< 0.0001.

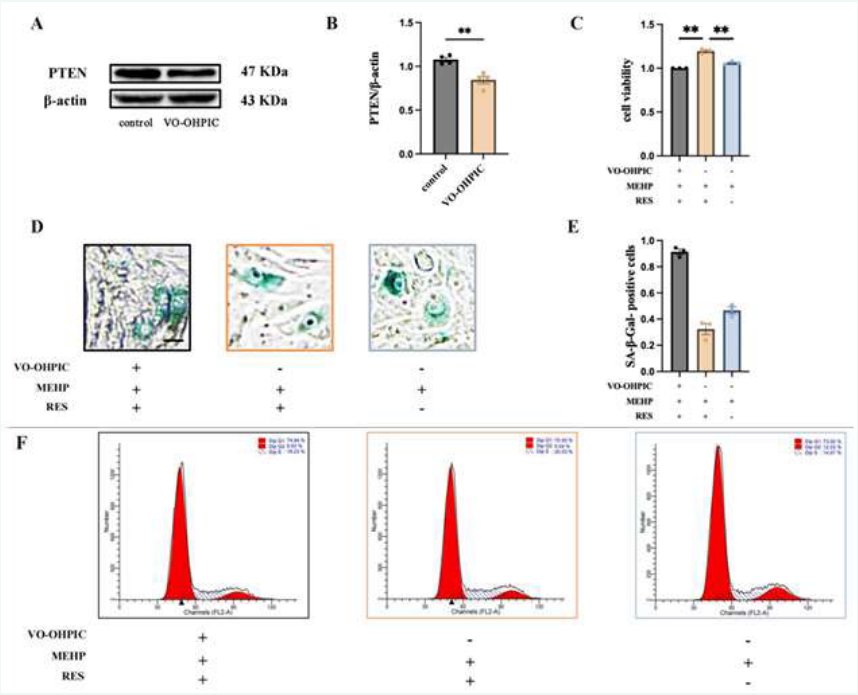

Figure 5: PTEN inhibition attenuated the protective effect of RES against MEHP in TM3 cells. The cells were processed to 1 μM inhibitor of PTEN (VO-Ohpic trihydrate), 200 μM MEHP and 2.5 μM RES for 24 h. **(A, B)** Analysis of the expressions of PTEN proteins. **(C)** Effect of PTEN inhibition on cell viability. **(D)** Evaluation of testosterone levels in TM3 cells culture supernatant. **(E, F)** The cell cycle distribution of TM3 cells. **(G, H)** SA-β-Gal stain results of TM3 cells (scale bar: 50 μm). **(I, J)** Analysis of the expressions of relevant senescence proteins in TM3 cells. The results are presented as mean±SEM. *P< 0.05, **P< 0.001, ***P< 0.0001. The results in F are presented as **P< 0.001, ##P< 0.001 vs. MEHP + RES group.

treatment group (Figure 5C). A pronounced increase in SA-β-Gal-positive cells in the VO-Ohpic-pretreated group compared to the MEHP+RES co-treatment group (Figure 5D, E). A significant elevation in the proportion of cells arrested in the G1 phase in the VO-Ohpic-pretreated group by flow cytometric analysis (Figure 5F, G). In the VO-Ohpic-pretreated group relative to the MEHP+RES co-treatment group, testosterone levels were significantly reduced (Figure 5H). Western blotting showed that VO-Ohpic treatment significantly upregulated β-Gal, p21, p16, and γH2AX compared to the co-treatment group (Figure 5I, J).

RES against MEHP-induced senescence through the PTEN–p-CHK2–CDK2 axis

To elucidate if this axis mediates RES protection, cells treated with VO-Ohpic were analyzed. Western blotting demonstrated that VO-Ohpic downregulated PTEN and CDK2 and upregulated p-CHK2, whereas MEHP+RES co-treatment reversed these alterations (Figure 6A-D). These results indicate that PTEN is essential for RES protection. Following PTEN inhibition, RES's protective effect was markedly attenuated. In summary, PTEN suppression triggers senescence via upregulation of p-CHK2 and

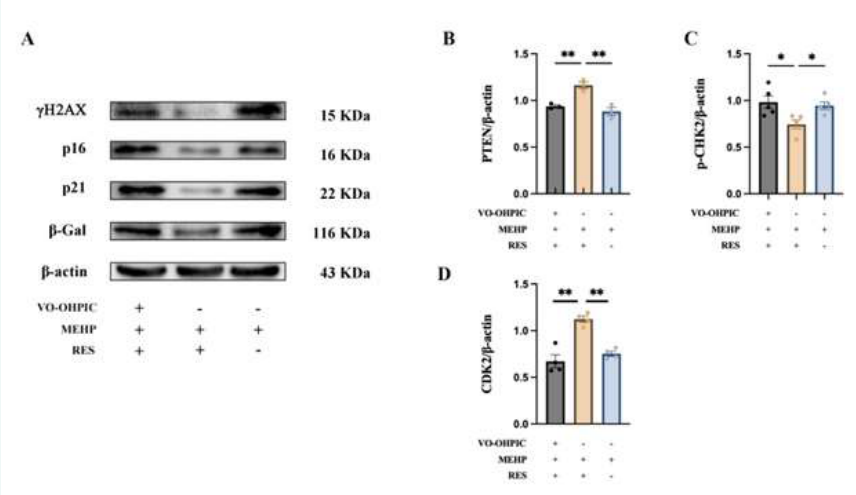

Figure 6: PTEN inhibition attenuated the protective effect of RES against MEHP in TM3 cells. The cells were processed to 1 μM inhibitor of PTEN (VO-Ohpic trihydrate), 200 μM MEHP and 2.5 μM RES for 24 h. **(A, B)** Analysis of the expressions of relevant signaling pathway proteins in TM3 cells. The results are presented as mean±SEM. *P< 0.05, **P< 0.001, ***P< 0.0001.

subsequent downregulation of CDK2. Under these conditions, RES cannot counteract MEHP-induced senescence without functional PTEN.

DISCUSSION

As a high-molecular-weight phthalate ester widely employed as PVC products, DEHP improves material flexibility and durability. Research has demonstrated that DEHP exposure exerts toxic effects across multiple organ systems, including the testes, ovaries, heart, and liver [38,39]. DEHP is categorized as a Group 2B probable human carcinogen by the International Agency for Research on Cancer (IARC). Moreover, prenatal exposure to DEHP has been linked to detrimental outcomes in offspring reproductive organ development, potentially causing reproductive dysfunction later in life [40,41]. Its primary metabolite, MEHP, exhibits even greater toxicity [42].

In animal studies, DEHP exposure disrupts the testicular barrier in male rats, leading to impaired spermatogenesis and decreased serum testosterone. Both DEHP and its metabolite MEHP exert detrimental effects on male reproductive function in rats, manifested as reduced testosterone synthesis, decreased sperm count, testicular cell damage, and compromised blood-testis barrier function in our prior investigations [2-43]. Building on this, the current study investigated the molecular mechanism of DEHP/MEHP-induced cellular senescence via PTEN loss and evaluated RES protection.

Cellular senescence, initially characterized by Hayflick and colleagues, represents a state of permanent and irreversible cell cycle arrest triggered by diverse forms of cellular stress [13]. This physiological and pathological process, distinct from apoptosis and necrosis, is characterized by proliferation cessation with maintained metabolic activity [44]. Hallmarks include structural degeneration, cell cycle arrest, biomolecular damage, metabolic dysregulation, and SASP development [45]. The primary forms of cellular senescence include: replicative senescence, driven by progressive telomere shortening; stress-induced premature senescence, triggered by DNA damage from reactive oxygen species (ROS), ultraviolet radiation, or chemical agents, and characterized by increased γH2AX expression; and developmental senescence, which occurs as a programmed process during embryogenesis [46,47].

Senescent cells exhibit characteristic changes. The lysosomal compartment expands, leading to enhanced activity of SA-β-Gal at an optimal pH of 6.0, which serves as a standard biomarker for identifying senescent cells [48]. Biomolecular damage involves oxidative and structural abnormalities in DNA, proteins, and lipids [49]. Activation of the p53/p21 and p16/Rb signaling pathways drives irreversible cell cycle arrest, a process that can be quantitatively assessed through flow cytometric analysis [50]. Metabolic reprogramming, including mitochondrial dysfunction and autophagy alterations, decreases cell viability [51,52]. Functionally, senescence induces tissue-specific impairments; for instance, diminished testosterone synthesis in senescent Leydig cells contributes directly to reproductive dysfunction [53].

In this research, DEHP exposure significantly declined testicular testosterone while upregulating p16, p21, γH2AX, and β-Gal, consistent with senescence (Figure 1). MEHP-induced senescence in TM3 cells was confirmed by CCK-8, flow cytometry, and SA-β-Gal staining (Figure 2).

PTEN, a crucial tumor suppressor that catalyzes the dephosphorylation of PIP3 dephosphorylation to negatively regulate the PI3K/AKT/mTOR signaling pathway [54,55]. PTEN loss causes pathway hyperactivation, inducing replication stress, DNA damage accumulation, and senescence via DDR activation [56,57]. Here, PTEN expression was significantly downregulated in testicular tissue and TM3 cells after DEHP/MEHP exposure. Mechanisms may involve transcriptional suppression, oxidative stress-mediated degradation, or impaired activity due to disrupted localization [58]. PTEN overexpression effectively suppressed MEHP-induced senescence (Figure 3).

RES exhibits a range of beneficial biological activities, including anti-inflammatory, antioxidant, cardioprotective effects, and the ability to activate the deacetylase SIRT1, which is a naturally occurring stilbenoid polyphenol [59,60]. In our system, RES co-treatment reversed DEHP/MEHP-induced PTEN downregulation (Figure1-5). The protective mechanism may involve regulation of E3 ubiquitin ligases (e.g., WWP2) to reduce PTEN ubiquitination/degradation, and/or enhancement of PTEN transcription via FOXO factors [61,62]. Using the PTEN inhibitor VO-OHpic, we found RES's anti-senescence effects were abolished when PTEN was inhibited, demonstrating its action depends on counteracting PTEN loss (Figure 5).

CHK2 is a pivotal cell cycle checkpoint kinase. Upon persistent DNA damage, the ATM/CHK2 pathway is chronically activated, phosphorylating CHK2 to produce p-CHK2, a biomarker of DNA damage [63,64]. CDK2, a cyclin-dependent kinase, depends on cyclin binding for activity. During DDR, activated p-CHK2 upregulates p21 via p53. p21, a broad-spectrum

CDK inhibitor, binds the CDK2-cyclin complex, inhibiting its kinase activity, which leads to G1/S arrest and even cellular senescence. Thus, reduced CDK2 activity indicates cell cycle arrest [65-72]. Our results suggest DEHP induces DNA damage via PTEN deficiency, activating ATM/CHK2 and elevating p-CHK2. Subsequently, CDK2 activity is suppressed via CDC25 phosphorylation and p21 induction, causing G1/S arrest and senescence. RES counteracts MEHP-induced senescence by modulating the PTEN/p-CHK2/CDK2 axis (Figure 4-6).

CONCLUSION

This research elucidated the molecular mechanism by which DEHP/MEHP leads to testicular cell senescence via promoting PTEN loss, activating p-CHK2, and inhibiting CDK2 activity. Furthermore, RES exerts anti-senescence effects by preserving PTEN function and maintaining homeostasis of the PTEN/p-CHK2/CDK2 signaling pathway. Theoretical basis for comprehending the reproductive toxicity of DEHP and lay an experimental groundwork for the development of potential preventive and therapeutic interventions.

DECLARATION OF COMPETING INTEREST

The authors declare that they have no known competing financial interests or personal relationships that could have appeared to influence the work reported in this paper.

ACKNOWLEDGMENTS

This work was supported by the National Natural Science Foundation of China (NSFC, 81872623), and Liaoning Provincial Natural Science Foundation of China (2023-MS-269). We acknowledge BioRender (https://biorender.com/) for providing scientific illustration tools. The figures in this paper were created using its platform.

CREDIT AUTHORSHIP CONTRIBUTION STATEMENT

Xinyu Yan: Writing – original draft, Investigation. Qing Tian: Formal analysis. Jiawei Xu: Data curation. Jiaxuan Ma: Conceptualization. Xiance Sun: Methodology. Jing Li: Methodology. Wang Ningning: Software. Yao Xiaofeng: Supervision, Software. Tianming Qiu: Visualization, Validation. Zhang Cong: Investigation. Deng Haoyuan: Supervision. Guang Yang: Writing – review & editing.

REFERENCES

1. Tuan Tran H, Lin C, Bui XT, Ky Nguyen M, Dan Thanh Cao N, et al. Phthalates in the environment: characteristics, fate and transport, and advanced wastewater treatment technologies. Bioresour Technol. 2022; 344: 126249.

2. Zhu Q, Zhai J, Chen Z, Guo Z, Sun X, Li J, et al. DEHP regulates ferritinophagy to promote testicular ferroptosis via suppressing SIRT1/PGC-1α pathway. Sci Total Environ. 2024; 954: 176497.

3. Li X, Fang EF, Scheibye-Knudsen M, Cui H, Qiu L, Li J, et al. Di-(2-ethylhexyl) phthalate inhibits DNA replication leading to hyperPARylation, SIRT1 attenuation, and mitochondrial dysfunction in the testis. Sci Rep. 2014; 4: 6434.

4. Huang HB, Cheng PK, Siao CY, Lo YC, Chou WC, Huang PC. Mediation effects of thyroid function in the associations between phthalate exposure and lipid metabolism in adults. Environ Health. 2022; 21: 61.

5. Zhang X, Yin Z, Xiang S, Yan H, Tian H. Degradation of Polymer Materials in the Environment and Its Impact on the Health of Experimental Animals: A Review. Polymers (Basel). 2024; 16: 2807.

6. Gorini F, Tonacci A, Sanmartin C, Venturi F. Phthalates and Non-Phthalate Plasticizers and Thyroid Dysfunction: Current Evidence and Novel Strategies to Reduce Their Spread in Food Industry and Environment. Toxics. 2025; 13: 222.

7. Matsuyama S, DeFalco T. Steroid hormone signaling: multifaceted support of testicular function. Front Cell Dev Biol. 2024; 11: 1339385.

8. Roychoudhury S, Chakraborty S, Choudhury AP, Das A, Jha NK, Slama P, et al. Environmental Factors-Induced Oxidative Stress: Hormonal and Molecular Pathway Disruptions in Hypogonadism and Erectile Dysfunction. Antioxidants (Basel). 2021; 10: 837.

9. Shulhai AM, Bianco V, Donini V, Esposito S, Street ME. Which is the current knowledge on man-made endocrine- disrupting chemicals in follicular fluid? An overview of effects on ovarian function and reproductive health. Front Endocrinol (Lausanne). 2024; 15: 1435121.

10. Peivasteh-Roudsari L, Barzegar-Bafrouei R, Sharifi KA, Azimisalim S, Karami M, Abedinzadeh S, et al. Origin, dietary exposure, and toxicity of endocrine-disrupting food chemical contaminants: A comprehensive review. Heliyon. 2023; 9: e18140.

11. Singh LK, Pandey R, Siddiqi NJ, Sharma B. Molecular Mechanisms of Phthalate-Induced Hepatic Injury and Amelioration by Plant-Based Principles. Toxics. 2025; 13: 32.

12. Chen S, Yu M, Yao Y, Li Y, He A, Zhou Z, et al. Thyroid Hormone Biomonitoring: A Review on Their Metabolism and Machine-Learning Based Analysis on Effects of Endocrine Disrupting Chemicals. Environ Health (Wash). 2024; 2: 350-372.

13. Nousis L, Kanavaros P, Barbouti A. Oxidative Stress-Induced Cellular Senescence: Is Labile Iron the Connecting Link? Antioxidants (Basel). 2023; 12: 1250.

14. Stallaert W, Taylor SR, Kedziora KM, Taylor CD, Sobon HK, Young CL, et al. The molecular architecture of cell cycle arrest. Mol Syst Biol. 2022; 18: e11087.

15. Kasperova BJ, Cinkajzlova A, Horvath L, Svoboda P, Haluzik M, Stemberkova et al. Coming of age: could obesity-related metabolic complications be treated by targeting senescent cells? Front Cell Dev Biol. 2025; 13: 1622107.

16. Hao X, Tu S, Pan D, Liao W, Yang L, Wang S, et al. Relationship of Ageing to Insulin Resistance and Atherosclerosis. Metabolites. 2025; 15: 613.

17. Sun R, Feng J, Wang J. Underlying Mechanisms and Treatment of Cellular Senescence-Induced Biological Barrier Interruption and Related Diseases. Aging Dis. 2024; 15: 612-639.

18. Li Y, Kang K, Bao H, Liu S, Zhao B, Hu G, et al. Research Progress on the Interaction Between SIRT1 and Mitochondrial Biochemistry in the Aging of the Reproductive System. Biology (Basel). 2025; 14: 643.

19. Wu Y, Shen S, Shi Y, Tian N, Zhou Y, Zhang X. Senolytics: Eliminating Senescent Cells and Alleviating Intervertebral Disc Degeneration. Front Bioeng Biotechnol. 2022; 10: 823945.

20. Chen B, Zhu R, Hu H, Zhan M, Wang T, Huang F, et al. Elimination of Senescent Cells by Senolytics Facilitates Bony Endplate Microvessel Formation and Mitigates Disc Degeneration in Aged Mice. Front Cell Dev Biol. 2022; 10: 853688.

21. Ouvrier B, Ismael S, Bix GJ. Senescence and SASP Are Potential Therapeutic Targets for Ischemic Stroke. Pharmaceuticals (Basel). 2024; 17: 312.

22. Varghese SS, Dhawan S. Senescence: a double-edged sword in beta-cell health and failure? Front Endocrinol (Lausanne). 2023; 14: 1196460.

23. Fu H, Zhu X, Di Q, Sun J, Jiang Q, Xu Q. m6A contributes to a pro-survival state in GC-2 cells by facilitating DNA damage repair: Novel perspectives on the mechanism underlying DEHP genotoxicity in male germ cells. Sci Total Environ. 2023; 859: 160432.

24. Hale A, Dhoonmoon A, Straka J, Nicolae CM, Moldovan GL. Multi-step processing of replication stress-derived nascent strand DNA gaps by MRE11 and EXO1 nucleases. Nat Commun. 2023; 14: 6265.

25. Yan F, Zhao Q, Li Y, Zheng Z, Kong X, Shu C, et al. The role of oxidative stress in ovarian aging: a review. J Ovarian Res. 2022; 15: 100.

26. Mohammed A, Atkin SL, Brennan E. Dysregulation of microRNA (miRNA) Due to Phthalate/Phthalate Metabolite Exposure and Associated Health Effects: A Narrative Review. J Xenobiot. 2025; 15: 72.

27. Dong S, Chen C, Zhang J, Gao Y, Zeng X, Zhang X. Testicular aging, male fertility and beyond. Front Endocrinol (Lausanne). 2022; 13: 1012119.

28. Álvarez-Garcia V, Tawil Y, Wise HM, Leslie NR. Mechanisms of PTEN loss in cancer: It's all about diversity. Semin Cancer Biol. 2019; 59: 66-79.

29. Alexandra T, Marina IM, Daniela M, Ioana SI, Maria B, Radu R, et al. Autophagy-A Hidden but Important Actor on Oral Cancer Scene. Int J Mol Sci. 2020; 21: 9325.

30. Yuan H, Liu J, Xu R, Yang K, Qu R, Liu S, et al. The spatiotemporal heterogeneity of reactive oxygen species in the malignant transformation of viral hepatitis to hepatocellular carcinoma: a new insight. Cell Mol Biol Lett. 2025; 30: 70.

31. Janic A, Abad E, Amelio I. Decoding p53 tumor suppression: a crosstalk between genomic stability and epigenetic control? Cell Death Differ. 2025; 32: 1-8.

32. Rasool R, Ullah I, Mubeen B, Alshehri S, Imam SS, Ghoneim MM, Alzarea SI, et al. Theranostic Interpolation of Genomic Instability in Breast Cancer. Int J Mol Sci. 2022; 23: 1861.

33. Mendonça ELSS, Xavier JA, Fragoso MBT, Silva MO, Escodro PB, Oliveira ACM, et al. E-Stilbenes: General Chemical and Biological Aspects, Potential Pharmacological Activity Based on the Nrf2 Pathway. Pharmaceuticals (Basel). 2024; 17: 232.

34. Yu X, Jia Y, Ren F. Multidimensional biological activities of resveratrol and its prospects and challenges in the health field. Front Nutr. 2024; 11: 1408651.

35. Neri S, Borzì RM. Molecular Mechanisms Contributing to Mesenchymal Stromal Cell Aging. Biomolecules. 2020; 10: 340.

36. Han D, Zhang QY, Zhang YL, Han X, Guo SB, Teng F, et al. Gallic Acid Ameliorates Angiotensin II-Induced Atrial Fibrillation by Inhibiting Immunoproteasome- Mediated PTEN Degradation in Mice. Front Cell Dev Biol. 2020; 8: 594683.

37. Wang Q, Yu Q, Wu M. Antioxidant and neuroprotective actions of resveratrol in cerebrovascular diseases. Front Pharmacol. 2022; 13: 948889.

38. Li X, Li C, Li Q, Wang Y, Yang M, Zhou Z, et al. Impact of prenatal Di(2-ethylhexyl) phthalate exposure on pubertal development in female offspring rats: A focus on ERα-Mediated IGF-1/NKB crosstalk in the hypothalamus. Sci Rep. 2025; 15: 22255.

39. Alam MS, Maowa Z, Hasan MN. Phthalates toxicity in vivo to rats, mice, birds, and fish: A thematic scoping review. Heliyon. 2024; 11: e41277.

40. Zeng F, Zhang L, Deng F, Lou S. Early-life exposure to di (2-ethyl-hexyl) phthalate: Role in children with endocrine disorders. Front Cell Dev Biol. 2023; 11: 1115229.

41. Wang J, Zhao C, Feng J, Sun P, Zhang Y, Han A, et al. Advances in understanding the reproductive toxicity of endocrine-disrupting chemicals in women. Front Cell Dev Biol. 2024; 12: 1390247.

42. Zhang X, Liu Y, Yi R, Sun X, Li J, Wang N, et al. Resveratrol: Great potential for alleviating di-2-ethylhexyl phthalate (DEHP)-induced testicular ferroptosis via the SIRT1-HIF-1α axis. Ecotoxicol Environ Saf. 2025; 303: 118933.

43. Zhang H, Ran M, Jiang L, Sun X, Qiu T, Li J, et al. Mitochondrial dysfunction and endoplasmic reticulum stress induced by activation of PPARα leaded testicular to apoptosis in SD rats explored to di-(2-ethylhexyl) phthalate (DEHP). Ecotoxicol Environ Saf. 2023; 268: 115711.

44. Yang H, Zhang X, Xue B. New insights into the role of cellular senescence and chronic wounds. Front Endocrinol (Lausanne). 2024; 15: 1400462.

45. Dominic A, Banerjee P, Hamilton DJ, Le NT, Abe JI. Time-dependent replicative senescence vs. disturbed flow-induced pre-mature aging in atherosclerosis. Redox Biol. 2020; 37: 101614.

46. Roger L, Tomas F, Gire V. Mechanisms and Regulation of Cellular Senescence. Int J Mol Sci. 2021; 22: 13173.

47. Childs BG, Durik M, Baker DJ, van Deursen JM. Cellular senescence in aging and age-related disease: from mechanisms to therapy. Nat Med. 2015; 21: 1424-1435.

48. Li YF, Ouyang SH, Tu LF, Wang X, Yuan WL, Wang GE, et al. Caffeine Protects Skin from Oxidative Stress-Induced Senescence through the Activation of Autophagy. Theranostics. 2018; 8: 5713-5730.

49. Ajoolabady A, Pratico D, Bahijri S, Tuomilehto J, Uversky VN, Ren J. Hallmarks of cellular senescence: biology, mechanisms, regulations. Exp Mol Med. 2025; 57: 1482-1491.

50. Hao H, Liang W, Zhang S, Cai X, Yakefu A, Gao S, et al. Ruxolitinib Delays Nucleus Pulposus Cell Senescence in Rat Intervertebral Discs. JOR Spine. 2025; 8: e70044.

51. Zhang F, Guo J, Yu S, Zheng Y, Duan M, Zhao L, et al. Cellular senescence and metabolic reprogramming: Unraveling the intricate crosstalk in the immunosuppressive tumor microenvironment. Cancer Commun (Lond). 2024; 44: 929-966.

52. Wang K, Gan M, Lei Y, Liao T, Li J, Niu L, et al. Perspectives on mitochondrial dysfunction in the regeneration of aging skeletal muscle. Cell Mol Biol Lett. 2025; 30: 94.

53. Xing D, Jin Y, Jin B. A narrative review on inflammaging and late-onset hypogonadism. Front Endocrinol (Lausanne). 2024; 15: 1291389.

54. Shorning BY, Dass MS, Smalley MJ, Pearson HB. The PI3K-AKT-mTOR Pathway and Prostate Cancer: At the Crossroads of AR, MAPK, and WNT Signaling. Int J Mol Sci. 2020; 21: 4507.

55. Bruno PS, Arshad A, Gogu MR, Waterman N, Flack R, Dunn K, et al. Post-Translational Modifications of Proteins Orchestrate All Hallmarks of Cancer. Life (Basel). 2025; 15: 126.

56. Piha-Paul SA, Tseng C, Leung CH, Yuan Y, Karp DD, Subbiah V, et al. Phase II study of talazoparib in advanced cancers with BRCA1/2, DNA repair, and PTEN alterations. NPJ Precis Oncol. 2024; 8: 166.

57. Parisotto M, Grelet E, El Bizri R, Dai Y, Terzic J, Eckert D, et al. PTEN deletion in luminal cells of mature prostate induces replication stress and senescence in vivo. J Exp Med. 2018; 215: 1749-1763.

58. Zhang Y, Park J, Han SJ, Yang SY, Yoon HJ, Park I, et al. Redox regulation of tumor suppressor PTEN in cell signaling. Redox Biol. 2020; 34: 101553.

59. Nijat D, Zhao Q, Abdurixit G, He J, Liu H, Li J. An Up-to-Date Review of Traditional Chinese Medicine in the Treatment of Atherosclerosis: Components, Mechanisms, and Therapeutic Potentials. Phytother Res. 2025; 39: 3709-3735.

60. El Oirdi M. Harnessing the Power of Polyphenols: A New Frontier in Disease Prevention and Therapy. Pharmaceuticals (Basel). 2024; 17: 692.

61. Wang Y, Liu J, Akatsu C, Zhang R, Zhang H, Zhu H, et al. LAPTM5 mediates immature B cell apoptosis and B cell tolerance by regulating the WWP2-PTEN-AKT pathway. Proc Natl Acad Sci U S A. 2022; 119: e2205629119.

62. Maddika S, Kavela S, Rani N, Palicharla VR, Pokorny JL, Sarkaria JN, et al. WWP2 is an E3 ubiquitin ligase for PTEN. Nat Cell Biol. 2011; 13: 728-733.

63. Lee YS, Doonan BB, Wu JM, Hsieh TC. Combined metformin and resveratrol confers protection against UVC-induced DNA damage in A549 lung cancer cells via modulation of cell cycle checkpoints and DNA repair. Oncol Rep. 2016; 35: 3735-3741.

64. Wang W, Liu H, Liu S, Hao T, Wei Y, Wei H, et al. Oocyte-specific deletion of eukaryotic translation initiation factor 5 causes apoptosis of mouse oocytes within the early-growing follicles by mitochondrial fission defect-reactive oxygen species-DNA damage. Clin Transl Med. 2024; 14: e1791.

65. Almansour BS, Binjubair FA, Abdel-Aziz AA, Al-Rashood ST. Synthesis and In Vitro Anticancer Activity of Novel 4-Aryl-3-(4-methoxyphenyl)-1-phenyl-1H-pyrazolo[3,4-b]pyridines Arrest Cell Cycle and Induce Cell Apoptosis by Inhibiting CDK2 and/or CDK9. Molecules. 2023; 28: 6428.

66. Fuentes-Antrás J, Bedard PL, Cescon DW. Seize the engine: Emerging cell cycle targets in breast cancer. Clin Transl Med. 2024; 14: e1544.

67. Barandiaran A, Montanes N, Sanchez-Nacher L, Balart R, Selles MA, Moreno V. Investigation of Cinnamic Acid Derivatives as Alternative Plasticizers for Improved Ductility of Polyvinyl Chloride Films. Polymers (Basel). 2023; 15: 4265.

68. Cheng H, Zhang X, Li Y, Cao D, Luo C, Zhang Q, et al. Age-related testosterone decline: mechanisms and intervention strategies. Reprod Biol Endocrinol. 2024; 22: 144.

69. Kaseke T, Lujic T, Cirkovic Velickovic T. Nano- and Microplastics Migration from Plastic Food Packaging into Dairy Products: Impact on Nutrient Digestion, Absorption, and Metabolism. Foods. 2023; 12: 3043.

70. Kumari R, Jat P. Mechanisms of Cellular Senescence: Cell Cycle Arrest and Senescence Associated Secretory Phenotype. Front Cell Dev Biol. 2021; 9: 645593.

71. Mohamad Kamal NS, Safuan S, Shamsuddin S, Foroozandeh P. Aging of the cells: Insight into cellular senescence and detection Methods. Eur J Cell Biol. 2020; 99: 151108.

72. Mouery BL, Baker EM, Mei L, Wolff SC, Mills CA, Fleifel D, et al. APC/C prevents a noncanonical order of cyclin/CDK activity to maintain CDK4/6 inhibitor-induced arrest. Proc Natl Acad Sci U S A. 2024; 121: e2319574121.